

● *Original Contribution***CHANGES IN ULTRASONIC DOPPLER BACKSCATTERED POWER
DOWNSTREAM OF CONCENTRIC AND ECCENTRIC STENOSES
UNDER PULSATILE FLOW**

GUY CLOUTIER, LOUIS ALLARD and LOUIS-GILLES DURAND

Laboratoire de Génie Biomédical, Institut de Recherches Cliniques de Montréal, Montréal, Québec, Canada

Abstract—The main objective of the present work was to investigate, under pulsatile flow, the patterns of variation of the Doppler power backscattered by blood and Sephadex particles upstream and downstream of concentric and eccentric stenoses ranging from 47% to 91% area reduction. Doppler measurements were performed at 5 diameters upstream and 5, 10, 15 and 20 diameters downstream of the constriction. For the concentric 75% and 85%, and the eccentric 79% and 91% area reduction stenoses, a progressive increase of the power backscattered by red cell suspensions at 40% hematocrit was measured downstream of the narrowing. The maximal power usually occurred around 10 diameters after the stenosis and dropped further downstream. In addition to the increase in the power, a cyclic variation of the backscattered intensity was observed within the flow cycle. For the concentric 52% and eccentric 47% area reduction stenoses, no variation of the Doppler power was measured during flow acceleration and deceleration for all recording sites. A coefficient of correlation of 0.82 was measured between the percentage of area reduction and the ratio of the Doppler mean power at 10 diameters downstream to that at 5 diameters upstream of the stenoses. Using Sephadex particles at low concentration, no increase of the Doppler power was found downstream of the 85% and 91% area reduction stenoses. The possible link between the intensity of turbulence and the power backscattered by blood is discussed along with the influence of the correlation between the scattering particles, under turbulent flow.

Key Words: Acoustics, Doppler effect, Ultrasonic tissue characterization, Ultrasonic blood characterization, Acoustic backscattering, Power mode, Arterial stenosis, Blood flow turbulence.

INTRODUCTION

In 1984, Shung et al. demonstrated that the presence of disturbed blood flow increased the power of the ultrasonic backscattered signal. In that study, red cells suspended in saline solution were circulated in a steady flow loop model and turbulence was generated by using a wire screen mesh. The ultrasonic signal backscattered by blood stirred in a container was also measured. In all experiments, the phenomenon of red cell aggregation was eliminated by using suspensions of red cells from which plasma proteins responsible for red cell aggregation were removed. In both series of measurements, the power of the ultrasonic A-mode signal increased for hematocrits greater than approximately 10%. It was then suggested that the backscattered power might be related to the turbulence intensity. Later, Bascom et al. (1988) investigated the effect of

varying the Reynolds number (Re) on the continuous-wave (CW) Doppler signal backscattered by a suspension of human red cells at 28% hematocrit, under steady flow. An increase of 38% of the amplitude of the signal was obtained at $Re = 1677$ (disturbed flow). Recently, the influence of flow turbulence on the pulsed-wave (PW) Doppler signal was also studied under steady flow using porcine red cells suspended in saline solutions at hematocrits varying between 2% and 40% (Shung et al. 1992). By circulating blood through a screen mesh, it was demonstrated that a relative turbulence intensity of 2.7% (as predicted by theory) significantly increased the Doppler backscattered signal for hematocrit values greater than approximately 10%. At 40% hematocrit, the increase was of the order of 2.8 dB. In the study by Shung et al. (1992), the relative turbulence intensity was defined as the ratio of the mean of the (velocity fluctuation)² by the (mean flow velocity)².

The effect of an asymmetrical 70% area reduction stenosis on the amplitude of the CW Doppler signal

Address correspondence to: Guy Cloutier, Laboratoire de Génie Biomédical, Institut de Recherches Cliniques de Montréal, 110 Avenue des Pins Ouest, Montréal, Québec H2W 1R7, Canada.

was recently studied under steady flow (Bascom et al. 1993). Using a suspension of red cells at 42% hematocrit, the Doppler power increased downstream of the stenosis to reach a maximum at about 6 to 10 diameters. At low hematocrit (4%), the onset of turbulence had little influence on the backscattered power. Using a pulsatile flow model, Cloutier and Shung (1992; 1993a) investigated the effect of turbulence promoted by passing blood through a screen mesh on the PW Doppler signal. In addition to an increase of 5.5 dB of the mean power backscattered by porcine red cell suspensions at 40% hematocrit, a variation of the amplitude of the signal was observed within the flow cycle. The power increased during flow acceleration to reach a maximum early after peak systole, and then decreased in diastole during flow deceleration.

In summary, three main observations are directly relevant to the present work: (1) the concentration of red cells has an influence on the backscattered power in turbulent flow; (2) the power varies as a function of the position downstream of a severe stenosis under steady flow; (3) the presence of turbulence promoted by a screen mesh induces a cyclic variation and an increase of the mean backscattered power under pulsatile flow.

Objectives of the research

The aim of the present work was to study the variation of the PW Doppler backscattered power upstream and downstream of concentric and eccentric stenoses, under pulsatile flow, using flow conditions similar to those found in the human circulatory system. The more specific objectives of the research were as follows:

1. To confirm that cyclic changes in the Doppler backscattered power exist downstream of severe vessel constrictions.
2. To evaluate if there is a correlation between the backscattered power and the percentage of area reduction.
3. To confirm that a low concentration of scatterers do not produce changes in the Doppler backscattered power, even downstream very severe stenoses.

MATERIALS AND METHODS

Ultrasonic scattering media

Fresh calf blood and superfine Sephadex particles (Sigma Chemical) of diameters ranging between 20 and 50 μm were used as ultrasonic scattering media. A 10% saline solution of ethylenediamine tetra-acetic acid dipotassium salt was mixed with blood at a concentration of 30 mL/L to prevent coagulation. Con-

centrated erythrocytes were obtained by centrifuging the whole blood at 2318 g (3000 RPM) for 30 min (Dacie and Lewis 1991) with an IEC PR-6000 centrifuge, and by removing the top white cell layer. The concentrated erythrocytes were washed and centrifuged twice with buffered 0.9% normal saline solution (pH 7.4). Each time the solution was centrifuged, the saline solution was aspirated to remove residual plasma proteins responsible for the aggregation of erythrocytes. This procedure was used even though bovine whole blood produces few if any aggregates at low shear rates (Schneck 1988). Before starting each experiment, blood was reconstituted by mixing the concentrated red cells with an isotonic normal saline solution (Celline™) to a hematocrit of 40%. Bovine albumin (Sigma Chemical) was added to the suspended red cells at a concentration of 0.5% to prevent crenation of erythrocytes. A microcentrifuge (Haemofuge, Heraeus Instruments) was used to measure the hematocrit by centrifuging the reconstituted blood over 10 min at 14,980 g (12,000 RPM). Since the pH may affect the volume of red cells (Dacie and Lewis 1991) and consequently the ultrasonic backscattered power (Shung et al. 1993), a Sentron pH meter (Model 1001) was used to measure the hydrogen-ion activity of the blood solution. In experiments performed using the Sephadex particles, the blood substitute was consisted of a solution of 40% glycerol and 60% saline by volume. The concentration of Sephadex was 2 g/L of solution. All experiments were performed at room temperature.

Pulsatile flow loop model

Experiments were performed in a closed flow loop model. The main flow conduit immersed horizontally in a water tank was a cylindrical 4.8-mm inner diameter silicone tube with a wall thickness of 1.6 mm. A rigid 4.8-mm inner diameter polyethylene tube was also used in one experiment. The length of the straight portion of the conduit was approximately 1 m. The silicone tube was selected in most experiments because a flexible conduit was needed to create the stenoses.

A reservoir of 1 L allowed filling of the *in vitro* model with blood or mixture of glycerol, Sephadex and saline solution. Continuous mixing of the solution was performed by a magnetic stirrer. A Harvard pulsatile blood pump (Model 1421) circulated the solution at a pulsation rate of 70 beats/min. The pulsation rate of the pump was monitored with a frequency counter (Fluke 87 True RMS Multimeter) triggered by the instantaneous pulsatile flow signal of an electromagnetic blood flowmeter (Cliniflow II, Model FM701D, Carolina Medical Electronics). A cannulating type flow probe (Model SF616) located 60 cm upstream of the

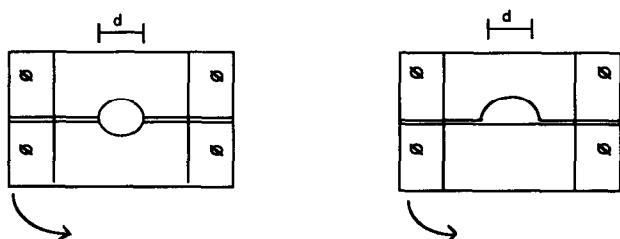


Fig. 1. Schematic representation of the strangling devices used to create concentric (left panel) and eccentric (right panel) stenoses.

stenosis on the main flow conduit was used with the flowmeter. The mean and maximal flow rates and the shape of the velocity waveforms were adjusted to correspond approximately to those observed in the human lower limb arterial system. The velocity waveforms were adjusted heuristically by modifying the compliance and resistance of the flow model. Since the minimal stroke volume of the Harvard pump was too high for our application, the flow output was divided between the main flow conduit and three parallel shunt tubes made of silicone. At the other end, the four tubes were joined together and immersed in the flow reservoir used to fill the model. Another tube was located between the reservoir and the input of the pump to close the loop.

Design of the constrictions

Few methods have been proposed to create artificial stenoses. Most of them have the disadvantage of changing permanently the diameter of the tube. Strangling devices simulating arterial stenoses of different area reduction were designed to simulate both concentric and eccentric vessel narrowing. Figure 1 shows a schematic representation of the strangling devices. The main advantage of this approach is that different stenoses can be introduced and removed quickly on the same tube. Each stenosis was calibrated using a video camera, a frame grabber and an image processing software installed in a Sun 386i computer. A light source illuminated the residual surface of the constricted tube from the bottom, at an angle of zero degree, and the camera positioned above the constriction detected the transmitted light. The residual surface was measured using the same light intensity for all stenoses. The focus of the camera was positioned at the center of the stenosis. The percentage of area reductions used in the present study were 52%, 75% and 85% for the concentric stenoses (31%, 50% and 61% reduction in diameter) and 47%, 79% and 91% for the eccentric stenoses. Figures 2 and 3 present examples of cross-

sectional and longitudinal views of the 75% concentric and 79% eccentric area reduction stenoses.

Ultrasonic Doppler measurements

Doppler backscattered power and blood flow velocity within the PW sample volume were measured with a 10-MHz system developed at Baylor College of Medicine, Houston, Texas. The angle between the tube and the Doppler probe was maintained at 60° for all measurements and the distance between the face of the 1.5-mm diameter nonfocused transducer and the location of the sample volume was kept constant at 1 cm. The position of the transducer instead of that of the gated echo was adjusted to maintain a constant sample volume for all measurements. At 1 cm from the face of the transducer, the diameters of the beam width were measured experimentally in water in two orthogonal directions using a hydrophone. The mean values were 1.27 mm at -3 dB and 1.78 mm at -6 dB. The beam profile was axially symmetric. The duration of the transmitted ultrasonic bursts was $0.8 \mu\text{s}$ and that of the gated returned echoes was $0.3 \mu\text{s}$, which provided a sample volume length of approximately 0.86 mm assuming a speed of ultrasound in blood of 1570 m/s (Evans *et al.* 1989). When using the water-glycerol solution, the length of the sample volume was slightly smaller.

Bandpass filtering of the received echoes between 200 Hz and 40 kHz was performed by the Doppler flowmeter. The frequency response of the Doppler system was characterized with a Brüel & Kjaer audio analyzer (Model 2012). The frequency response of the flowmeter operating at a pulse repetition frequency (PRF) of 62.5 kHz was calibrated by removing the audio board. Sine wave signals having an amplitude and dc offset similar to that provided by the radio-frequency (RF) board, when using blood as scattering medium, were used to drive the audio circuitry between 10 Hz and 31.25 kHz. These signals were sampled at 62.5 kHz by the sample-and-hold amplifier. Signals with a higher amplitude were also used to test the

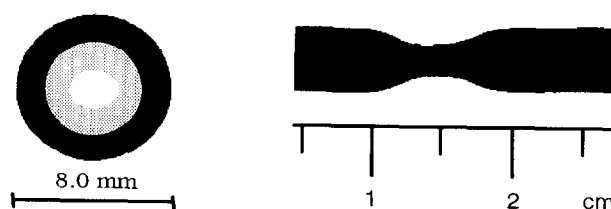


Fig. 2. Cross-sectional and longitudinal views of the concentric 75% area reduction stenosis in a 4.8-mm inner diameter (8.0-mm outer diameter) silicone tube.

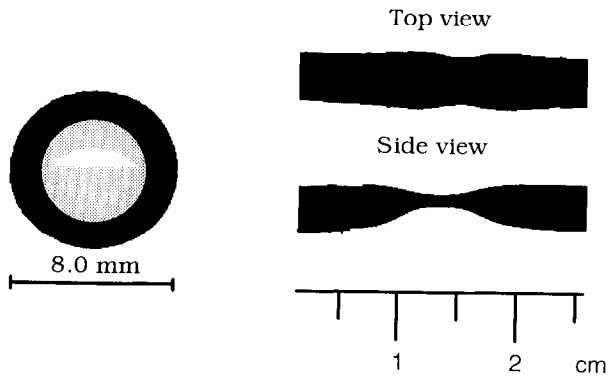


Fig. 3. Cross-sectional and longitudinal views of the eccentric 79% area reduction stenosis in a 4.8-mm inner diameter (8.0-mm outer diameter) silicone tube.

linearity of the system. The sensitivity of the audio analyzer was set at 0.1 dB. Figure 4 shows the frequency response of the Doppler system. The response was within 0 to -3 dB between approximately 400 Hz and 15.5 kHz. The frequency response was linear since it was not affected by a change of the input amplitude [20 and 500 mV root mean square (RMS)]. To ensure that the frequency response did not create artifact in the backscattered power estimation, numerical compensation was carried out before computing the spectrogram to obtain a flat bandwidth between 10 Hz and PRF/2. During the calibration of the Doppler system, the frequency responses of the Doppler transducer and RF board were not taken into consideration. Since Doppler probes usually have a low quality factor (large bandwidth) and because the bandwidths of the receiver and demodulator are inversely proportional to the axial resolution of the system (Evans et al. 1989), the contribution of these factors is expected to be nonsignificant.

Before starting Doppler measurements, blood and the water-glycerol solution were circulated in the model for approximately 2 h to eliminate air bubbles. The selected stenosis was then positioned on the tube and the gate output signal of the Doppler system was monitored with a Hewlett-Packard digitizing oscilloscope (Model HP-54503A) to allow accurate positioning of the sample volume. The position of the near and far walls of the tube was determined by listening to the audio Doppler signals. Measurements were performed at several locations upstream and downstream of the stenosis. The sample volume of the Doppler system was located at the center of the tube for all experiments. Backscattered power and velocity measurements were made at 5 tube diameters upstream of the stenosis and at 5, 10, 15 and 20 diameters downstream.

Data acquisition, signal processing and spectral analysis

The Doppler in-phase (I) and quadrature (Q) components, and the flow signal obtained from the electromagnetic flowmeter were digitized for 48 s at sampling rates of 50 kHz and 500 Hz, respectively. A PC-compatible 250 kHz and 12-bit resolution digitizing board (Data Translation, Model DT-2821G-SE) was used to sample the signals (gain = 8). A software program written in C allowed digitization of the signals over 50 consecutive flow cycles directly into the extended memory of the computer. From the digitized data stored on hard disk, another C program allowed computation of a mean spectrogram. A cross-correlation algorithm applied to the electromagnetic flowmeter signal was used to locate and synchronize the beginning of each cycle.

Time-frequency representations of the Doppler signal were obtained using autoregressive (AR) modeling. Based on previous studies (Kaluzynski 1987; Vaitkus et al. 1988; Guo et al. 1994), this algorithm may provide less variance in the spectral estimate than the Fourier representation. The visual inspection of the results of one experiment showed a lower variability in the Doppler power estimation when using AR modeling. This algorithm was then preferred to the Fourier algorithm. The Yule-Walker equations together with the Levinson-Durbin method were used to compute the AR spectrograms. Rectangular 14-ms windows were applied to the I and Q Doppler signals and a Doppler spectrum was computed at each time interval of 5 ms. Based on a previous simulation study (Guo

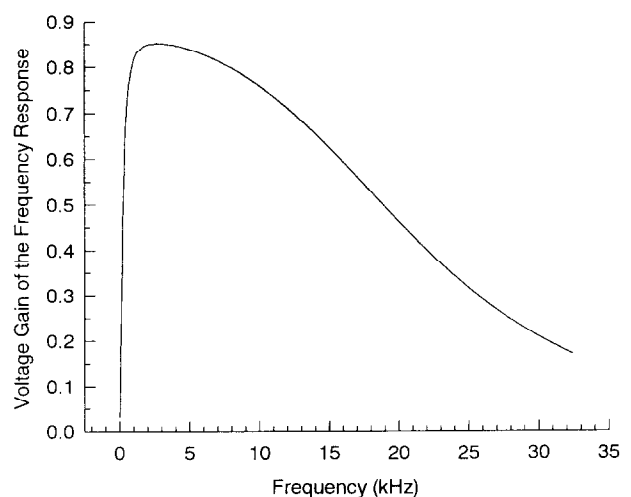


Fig. 4. Amplitude of the frequency response of the audio circuitry of the Doppler flowmeter for a sampling frequency of 62.5 kHz.

et al. 1994), these parameters provided the best fit between the computed spectrogram and the simulation of a theoretical spectrogram corresponding to the flow in the femoral artery. The Doppler time-frequency distributions were computed over 50 cycles for each experiment and averaged to obtain a mean representation of the frequency content of the signal over a flow cycle. The "Akaike's information criterion" (Akaike 1974) was used to determine the optimal number of poles for each windowed segment of 14 ms of the signal. The maximal number of poles was limited to 12.

In some experiments, even though care was taken to eliminate sources of air bubbles, spurious high-amplitude backscattered echoes of short duration were observed on the temporal in-phase and quadrature components. The algorithm described next was used to eliminate these artifacts.

The mean and standard deviation (SD) of the Doppler backscattered RMS amplitude were first computed from each segment of 14 ms of the I and Q temporal signals. Approximately 8600 segments were included in the computation of the statistical values for each component of the signal (50 cycles of 0.86 s/5-ms lag between each segment). Since the Doppler signal is known to be Gaussian, even in the case of turbulent flow when a short data window is used (Bascom et al. 1993), the statistical distribution of the RMS amplitudes is also approximated by the Gaussian distribution for $n > 30$. Consequently, all segments having an RMS amplitude higher or smaller than the mean ± 3 SD were excluded from the computation of the mean spectrogram. Theoretically, the probability that the RMS amplitudes are included within the mean ± 3 SD is 0.9974. In all experiments performed with concentric stenoses, only $0.9 \pm 0.4\%$ of the segments were eliminated because of the presence of air bubbles. In the cases of eccentric stenoses, the percentage of rejection was $0.7 \pm 0.6\%$. Even though these numbers are very small, eliminating those segments significantly reduced the variability of the Doppler backscattered power estimation.

The following equation was used to compute the mean power P of each Doppler spectrum included in the mean spectrogram:

$$P = 1 / NFFT \sum_{f_k=0}^{NFFT} P(f_k), \quad (1)$$

where $P(f_k)$ represents the power at frequency f_k and $NFFT$ the number of samples of each spectrum ($n = 1024$). Since low-frequency vibrations (clutter) were artificially introduced in all over the flow cycles when

Table 1. Experimental conditions for the flow loop experiments.

	Concentric stenoses	Eccentric stenoses
Mean flow	153 \pm 3 mL/min	150 \pm 7 mL/min
Peak flow	436 \pm 21 mL/min	422 \pm 25 mL/min
Hematocrit	39.3 \pm 1.1%	40.1 \pm 0.7%
pH	7.1 \pm 0.1	7.10 \pm 0.04

compensating the frequency response of the Doppler flowmeter (amplification of the noise between 10 Hz and the wall filter frequency), frequencies between 0 Hz and ± 195 Hz were set to zero before computing the backscattered power.

RESULTS

In experiments using blood, all measurements were repeated five times on different days and with different blood samples. Table 1 summarizes the experimental conditions selected for both series of measurements using concentric and eccentric stenoses. The mean and peak flows obtained from the electromagnetic flowmeter were averaged over 50 cycles for each recording. To determine the reproducibility of the adjustment of the flow waveform between each measurement, these mean values were averaged over the five recording sites (5 diameters upstream and 5, 10, 15 and 20 diameters downstream of the stenosis) and over the five experiments ($n = 25$). It is the statistics of these last values that are reported in Table 1. The hematocrit and pH were averaged over five experiments. Within a given day of measurements, both variables were measured first at the beginning and also at the end of the experiment. Few variations were noted in the hematocrit while the pH was constant.

Doppler backscattered power from blood

Figure 5 shows the pattern of the time variations of the Doppler backscattered power upstream and downstream of the concentric 85% area reduction stenosis. The mean velocity within the Doppler sample volume recorded 5 diameters (D) upstream of the stenosis is also shown for time reference. Upstream of the stenosis (-5 D), no variation of the Doppler backscattered power was observed during flow acceleration and deceleration. A reduction of the power was found at the end of diastole before the acceleration of the flow. However, since frequency components below 195 Hz (3 cm/s) were eliminated because of the clutter, this reduction may be artificial. Downstream of the stenosis, a cyclic variation and an increase of the backscattered power were observed at each recording site.

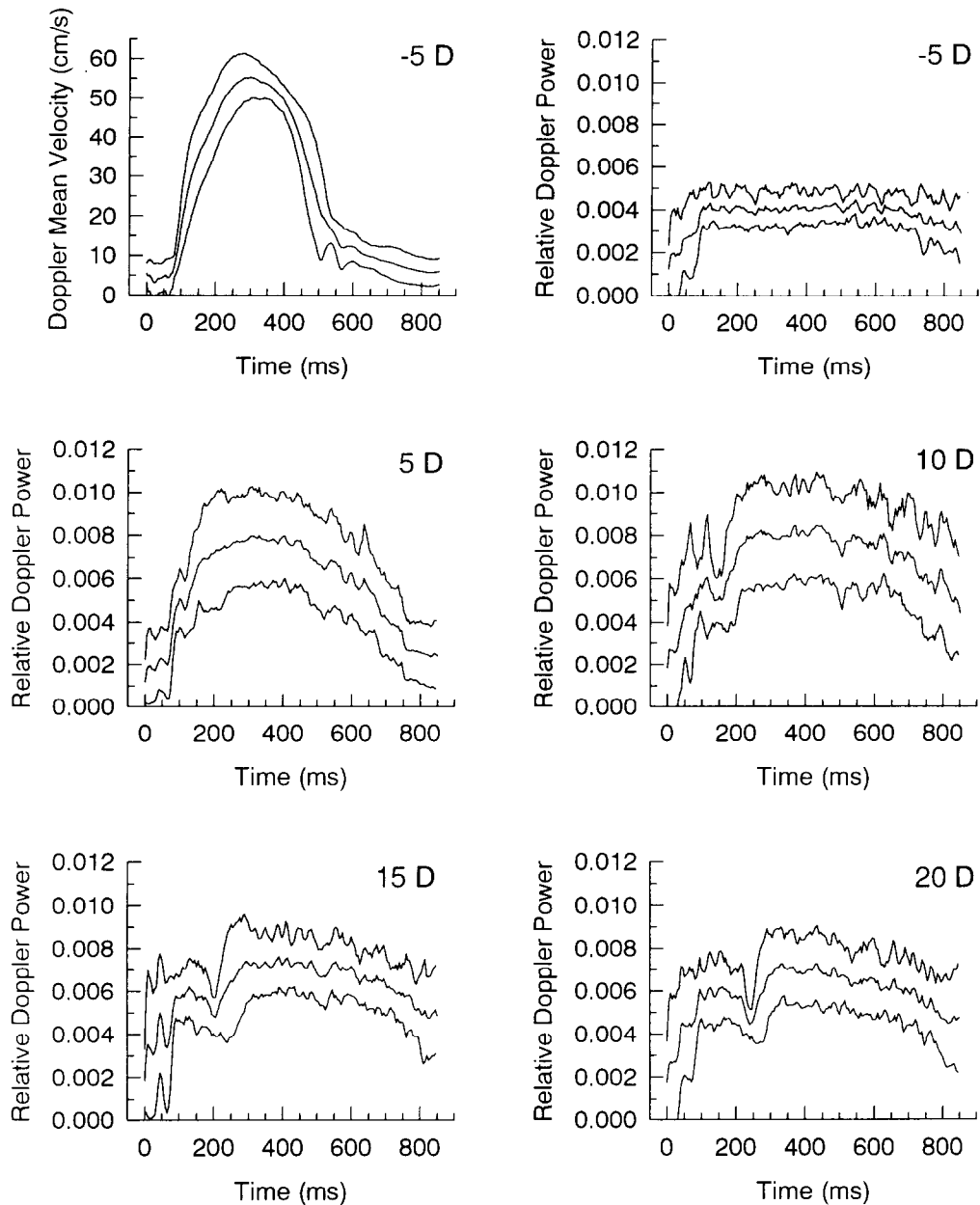


Fig. 5. Mean \pm SD of the averaged velocity within the Doppler sample volume located 5 diameters upstream of the concentric 85% area reduction stenosis (top left panel). Other panels show the mean \pm SD of the relative Doppler power backscattered by calf red cell suspensions at 40% hematocrit for the PW sample volume located at 5 diameters upstream (-5 D), and 5, 10, 15 and 20 diameters downstream of the stenosis. The statistical means and SDs were computed over five experiments. For each experiment, the backscattered power was measured from the mean spectrogram averaged over 50 cycles.

Similar patterns of variation of the Doppler power were also found for the concentric 75%, and eccentric 79% and 91% area reduction stenoses. The power was relatively constant downstream of the concentric 52% and eccentric 47% area reduction stenoses.

To better quantify these changes the mean power

averaged over the flow cycle was computed for each recording site and averaged over five experiments. The SD was also evaluated to provide an information on the cyclic variation of the backscattered power within the flow cycle. In the evaluation of the means and SDs, approximately 172 samples were included for each ex-

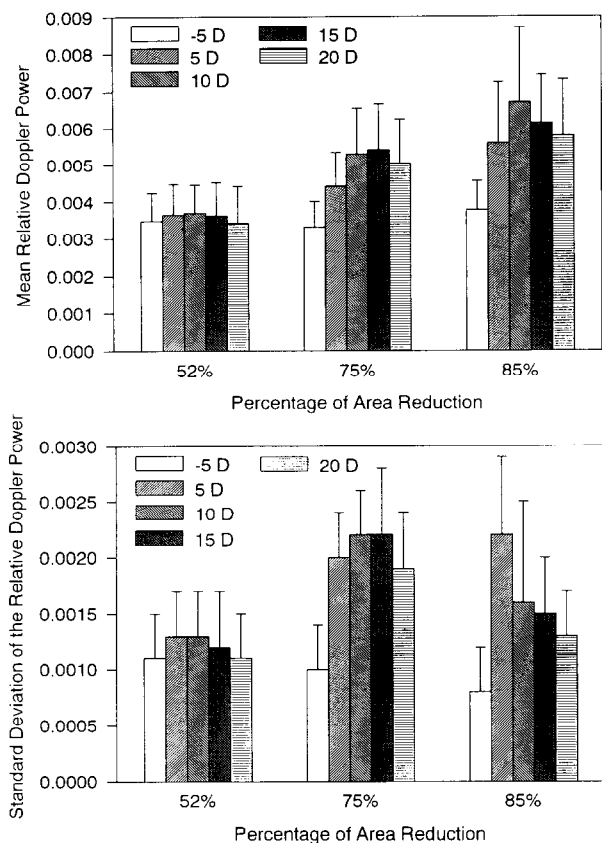


Fig. 6. Mean and SD over the flow cycle of the Doppler backscattered power computed from the mean spectrogram of signals recorded upstream and downstream of concentric stenoses. The mean relative Doppler power (top panel) provides information about the averaged power within the flow cycle, while the standard deviation (bottom panel) provides information on the cyclic variation of the Doppler backscattered power. The errors on the bar graphs are the SDs computed over five experiments.

periment (cycles of 0.86 s/5-ms interval between each sample). The results for the concentric stenoses are presented in Fig. 6, while those for the eccentric stenoses are shown in Fig. 7. The SDs on the bar graph were evaluated from five experiments.

For both concentric and eccentric stenoses, the variation of the mean Doppler power as a function of the position from the stenosis was similar. No increase of the mean power was measured downstream of the concentric 52% and eccentric 47% stenoses. However, the power increased progressively downstream of the more severe stenoses (75% to 91%) to reach a maximum at 10 or 15 D depending on the stenosis. For these last stenoses, the power at 20 D was always lower than that measured just proximally at 15 D, but higher than the value at -5 D. An interesting change in the cyclic variation of the Doppler

backscattered power was observed after vessel narrowing with 75% to 91% area reduction. Generally, the cyclic variation increased rapidly and decreased progressively further downstream. Two additional observations can be made from Figs. 6 and 7. First, a positive correlation seems to exist between the mean Doppler power and the percentage of area reduction. No such correlation appears to be present between the cyclic variation of the Doppler backscattered power and the severity of the stenosis.

Correlation between the mean backscattered power and the severity of the stenosis

For each experiment, the ratio of the mean power at 10 D to that at -5 D was computed and correlated with the percentage of area reduction, independently of the shape of the constriction. Power ratios were used

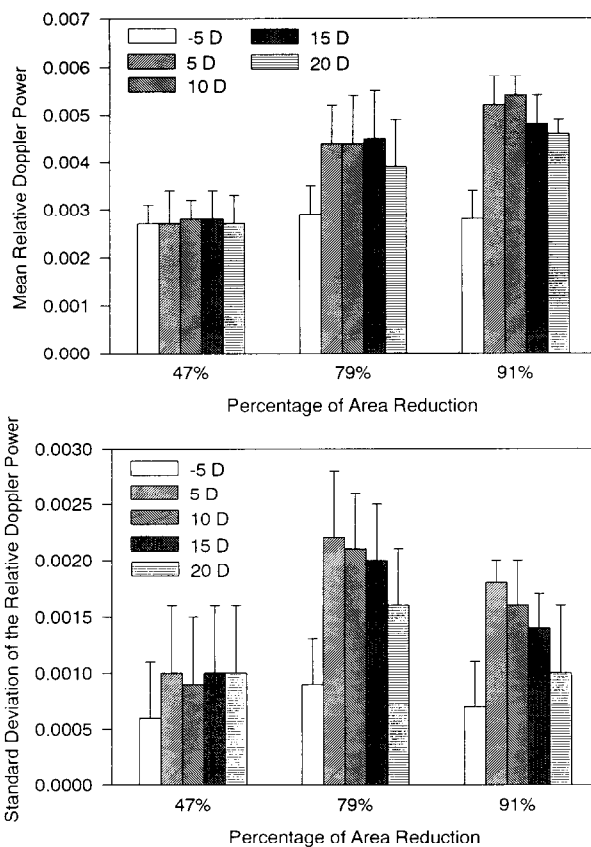


Fig. 7. Mean and SD over the flow cycle of the Doppler backscattered power computed from the mean spectrogram of signals recorded upstream and downstream of eccentric stenoses. The mean relative Doppler power (top panel) provides information about the averaged power within the flow cycle, while the SD (bottom panel) provides information on the cyclic variation of the Doppler backscattered power. The errors on the bar graphs are the SDs computed over five experiments.

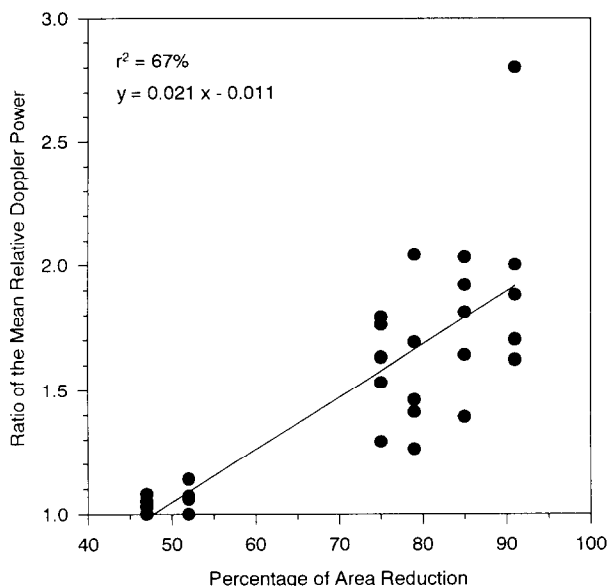


Fig. 8. Coefficient of determination (r^2) between the percent area reduction and the Doppler mean power at 10 diameters downstream of the stenosis divided by that 5 diameters upstream. Each point corresponds to an experiment performed with different blood samples.

to eliminate the effect of the variation in echogenicity between blood samples. A coefficient of correlation (R) of 82% (coefficient of determination $r^2 = 67\%$) was obtained, as shown in Fig. 8. The correlation was lower for the other power ratios tested: 5 D/-5 D, 15 D/-5 D and 20 D/-5 D.

Doppler backscattered power from Sephadex particles

A series of measurements using Sephadex particles was performed upstream and downstream of the concentric 85% and eccentric 91% area reduction stenoses. No power increase was observed downstream of both severe stenoses. The patterns of variation of the backscattered power were similar for all recording sites (-5 D, 5 D, 10 D, 15 D and 20 D). As seen in Fig. 9, the Doppler power was constant for most duration of the flow cycle and dropped at the end of diastole until the beginning of the acceleration of the flow.

DISCUSSION

Analysis of the results

A sudden reduction of the backscattered power was observed before peak systole downstream of the 75% to 91% area reduction stenoses. As seen in Fig. 5, a notch in the backscattered power mean curve was present 115 ms after the beginning of the cycle for measurements at 5 D, and at 145, 205 and 240 ms for

measurements performed at 10, 15 and 20 D after the stenosis. For the other stenoses, the timing slightly differed but the notches always occurred first at 5 D, then at 10 D, 15 D and 20 D. The mean duration between two notches occurring 5 D apart was 46 ± 14 ms, which corresponds to a propagation speed of 52 cm/s.

The exact mechanism involved in this sudden reduction of the backscattered power during the acceleration of blood is unknown. In a previous study on the cyclic variation of the Doppler power backscattered by blood under turbulent flow (Cloutier and Shung 1993a), no such sudden loss of the signal power was observed. However, a rigid polyethylene tube was used and turbulence was produced by introducing a grid in the flow model. An additional experiment was thus performed in the present study to test the possible influence of the dilatation of the silicone tube on the Doppler backscattered power. Measurements were performed downstream of a permanent severe stenosis molded in a rigid polyethylene tube using red cell suspensions at 39% hematocrit. Similar notches were observed eliminating the tube compliance as a possible cause of this phenomenon. In addition, the Doppler power reduction cannot be attributed to the disaggregation of red cells (Cloutier and Shung 1993b), since calf red cells washed twice and resuspended in saline solution were used in the current study. It is thus postulated that the sudden reductions of the backscattered power may be related to rapid changes in the character-

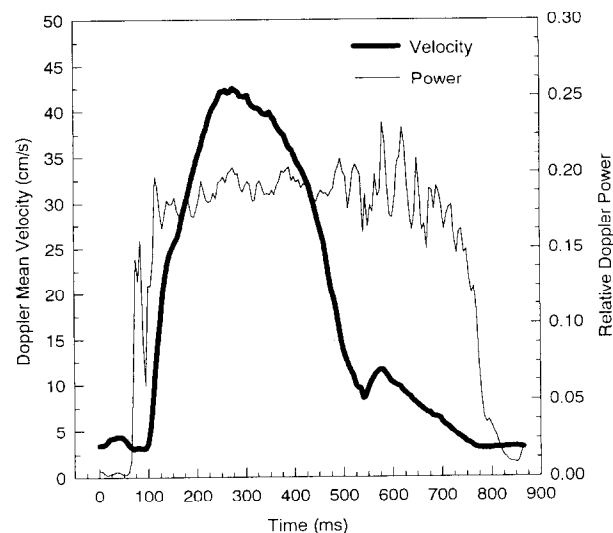


Fig. 9. Mean velocity within the Doppler sample volume located 10 diameters downstream of the eccentric 91% area reduction stenosis, and the relative Doppler power. Sephadex particles in a mix of saline water and glycerol were used as the ultrasonic scattering medium.

istics of the turbulence propagation along the tube during the acceleration of blood. Further investigations will be needed to elucidate the mechanisms involved in the Doppler power reductions.

For both mean and cyclic power presented in Figs. 6 and 7, a rapid increase followed by a progressive reduction of the intensity was observed downstream of the more severe stenoses. It was interesting to observe that the same patterns of variation were present for each individual experiment. Consequently, the errors shown on the bar graph are a result not only of the random fluctuations of the measurements, but also of the variation in the echogenicity between each blood sample. To eliminate this last effect, the ratio of the mean power at 10 D to that at -5 D was computed in the evaluation of the correlation between the backscattered power and the severity of the stenosis. As shown in Fig. 8, the variability was very low for the 47% and 52% stenoses and higher for the more severe constrictions.

A few reasons may explain the variability shown in Fig. 8 and consequently the moderate correlation value of 82% obtained: (1) the variance of power ratios is twice that of the individual parameters; (2) the variability in reproducing the same severity of area reduction for the more severe stenoses; (3) the intrinsic variability of turbulent flow and (4) the measurement of the maximal power that was probably not exactly at 10 D for all stenoses. Using a larger sample volume to increase the averaging of the turbulence intensity could decrease the variance of the results and increase the correlation. The selection of a lower transmitted frequency may have a similar effect because averaging is increased by reducing the spatial resolution of the measurement system. Reducing the frequency of the ultrasonic beam and consequently the spatial resolution could, on the other hand, affect the sensitivity of the method in detecting low intensity of blood flow turbulence (small velocity fluctuations).

Comparison of the results with those found in the literature

As shown in the examples of Fig. 5, the backscattered power was constant during flow acceleration and deceleration upstream of all stenoses studied and downstream of the 47% and 52% vessel narrowing. This is in accordance with our previous study (Cloutier and Shung 1993a) that showed no power variation during flow acceleration and deceleration under laminar flow for mean Doppler velocities ranging between 15 to 90 cm/s.

Under turbulent flow produced by a grid (Cloutier and Shung 1993a), the backscattered power varied

within the flow cycle and the maximum occurred during the deceleration of blood. A difference of 5.5 dB of the power (3.5 times) was observed between laminar and turbulent flow experiments. In the present study, a cyclic variation of the Doppler power was also present downstream of the 75% to 91% stenoses. The maximal increase of the backscattered power between laminar (-5 D) and turbulent flow (10 D) ranged between 1.25 and 2.8, which is lower than the power increase of 3.5 measured with the grid suggesting that the turbulence intensity was probably lower in the current study. Figure 5 shows that the backscattered power was maximal around peak systole at 5 D, while a plateau was generally observed between peak systole and the end of flow deceleration for measurements at 10, 15 and 20 D. This last observation seems to be in accordance with hot-film anemometer measurements of turbulence intensity done by others (Clark and Schultz 1973; Falsetti *et al.* 1983; Hanai *et al.* 1991). In these studies, turbulence started around peak systole or earlier and continued during flow deceleration.

In a previous steady flow experiment performed using a suspension of red cells at 42% hematocrit, Bascom *et al.* (1993) observed a progressive increase of the backscattered power downstream of an asymmetrical 70% area reduction stenosis, a peak at approximately 10 D after the stenosis, and a reduction further downstream. The power at 22 D was slightly higher than that measured 5 D upstream of the stenosis. In the present study, similar patterns of variation of the backscattered power were measured for stenoses between 75% and 91% area reduction, using a pulsatile flow model. In the study by Bascom *et al.* (1993), the power increased by a factor of approximately 1.5 between 5 D upstream and 10 D downstream of the 70% area reduction stenosis. From the regression analysis presented in Fig. 8, the power increase would be 1.48 for a 70% area reduction stenosis, which is similar to the results by Bascom *et al.* (1993) even if different mean flows (307 mL/min vs. 151 mL/min), transmitted frequencies (5 MHz vs. 10 MHz) and modalities (CW vs. PW Doppler) were used in both studies.

Relationship between turbulence and Doppler backscattered power

The relationship existing between the observation of turbulence downstream of a stenosis (Young 1979; Clark 1980; Giddens *et al.* 1993) and the location of the maximal ultrasound backscattered power observed in Figs. 6 and 7 or in the study by Bascom *et al.* (1993), suggests that power measurements may provide an index of the intensity of turbulence.

Several factors are known to influence the inten-

sity of the ultrasound signal backscattered by blood (Shung et al. 1993). It is understood that the transmitted frequency, the volume of the scatterers, the presence of red cell aggregation, the compressibility and density of red cells and plasma, the hematocrit, and the packing factor (Twersky 1988; Berger et al. 1991), which is a measure that considers the interaction among red cells, can influence the intensity of the Doppler backscattered signal. In the present study, most variables were constant within an experiment and the changes in the Doppler power are thus only attributed to the variation of the packing factor.

The influence of blood flow turbulence on the variation of the packing factor is difficult to predict. The reduction of the correlation between red cells in turbulent flow is certainly a major determinant contributing to the increase in the backscattered power. Previous studies (Shung et al. 1984; 1992) showed that the variation of the hematocrit between 20% and 40% had no visible effect on the difference between the ultrasonic backscattered power measured in laminar and turbulent flows. On the other hand, both hematocrit and red cell deformability were shown to influence the intensity of turbulence, as reported in the following three studies. In the experiments performed by Munter and Stein (1974) and Stein and Sabbah (1975), the intensity of turbulence measured with a hot-film anemometer was greater at hematocrits between 20% and 30% than that of plasma having similar viscosity and density. Surprisingly, at 40% hematocrit the turbulence intensity was similar to that of viscous plasma. Reynolds numbers ranging between 200 and 600 were used in those experiments and turbulence was induced by introducing a tube constriction in the *in vitro* model. In another series of experiments, performed at Reynolds numbers between 400 and 1400 (Sabbah and Stein 1976), hardened red cells obtained by gluteraldehyde fixation generated a level of turbulence consistently higher than that of blood composed of an equal number of fresh normal cells.

These last studies may generate new hypotheses on factors contributing to the variation of the backscattered power under turbulent flow. Since the turbulence intensity is reduced at 40% hematocrit and because the backscattered power is not significantly modified, one may postulate that the reduction of the turbulence intensity is compensated by an increase in the correlation among red cells as the hematocrit is increased between 30% and 40%. Additional experiments will be needed to better understand the relation between the hematocrit, red cell deformability, the intensity of turbulence and the ultrasound backscattered power.

Clinical implication

Currently, duplex scanning and color Doppler imaging (Evans et al. 1989; Strandness 1990) provide an accurate quantification of the severity of hemodynamically significant stenoses (>75% in area reduction). The method described in the present study does not seem better than any other ultrasound modalities presently available to clinicians. However, as discussed below, it is believed that it may in the future provide a better quantification of the intensity of blood flow turbulence than Doppler spectral broadening.

The strong spectral broadening observed by clinicians when positioning the PW Doppler sample volume in the poststenotic jet has been attributed for many years to the presence of blood flow turbulence. However, it is known from fluid mechanics studies (Young 1979; Clark 1980) that turbulence is developed after severe stenoses when the vortices in the jet begin to break down. The significant broadening observed in the jet is probably due mainly to strong velocity gradients and not only to turbulence (Jones 1993). In the study by Garbini et al. (1982a; 1982b), the turbulence intensity measured with a hot-film anemometer was

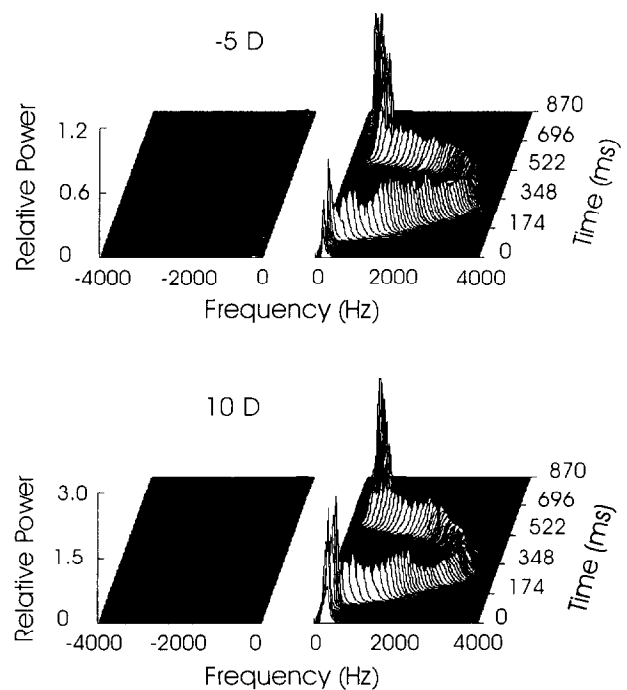


Fig. 10. Examples of mean Doppler spectrograms recorded 5 diameters upstream (top panel) and 10 diameters downstream (bottom panel) of the eccentric 91% area reduction stenosis. The ratio of the backscattered power at 10 D to that at -5 D was 2.0 (3 dB increase). No significant spectral broadening was observed 10 diameters downstream of the stenosis.

correlated with the broadening of the spectra for Reynolds numbers ranging between 6000 and 40,000. Turbulence levels between 3% and 4.5% could be accurately estimated from the measurement of spectral bandwidths. However, the broadening was small as compared to that observed in the jet of severe stenoses. Moreover, transit-time effects (intrinsic broadening) limited the applicability of the technique to lower intensities of turbulence.

In the present study, spectral broadening was observed in the jet and at 5 diameters downstream of severe stenoses. Between 10 and 20 D downstream of the stenosis, no broadening was found even if turbulence was detected by an increase of the backscattered power (see Fig. 10). As observed in the study by Bascom *et al.* (1993), the maximal Doppler power increase always occurred in regions where spectral broadening was small. This may suggest that Doppler power measurements may be more sensitive to turbulence than Doppler spectral broadening.

CONCLUSION

It has been demonstrated that both concentric and eccentric severe stenoses produced turbulence levels detectable by Doppler backscattered power measurements. For the 75% to 91% area reduction stenoses, a progressive increase of the power was found after the stenosis followed by a drop further downstream. The maximal backscattered power occurred usually at 10 D downstream of the stenosis. At 20 D, the amplitude of the Doppler signal was still higher than that measured 5 D before the constriction. In addition to the increase of the Doppler power averaged within the flow cycle, a cyclic variation of the backscattered intensity was observed between 5 D and 20 D downstream of the severe stenoses. Upstream of all stenoses included in the study and also downstream of the 47% and 52% area reduction stenoses, the power was constant during the acceleration and deceleration of red cells.

In conclusion, our study reinforces the hypothesis that the ultrasonic backscattered signal is correlated with the intensity of turbulence. The current belief that the correlation among the scattering particles under disturbed flow is a main determinant affecting the intensity of the backscattered signal is also supported by our work. Some companies are currently offering their own version of the color-Doppler power modality (*e.g.*, Diasonics, ATL, Toshiba, Acuson, Interspec). A complete knowledge of all factors affecting the backscattering of Doppler ultrasound from blood is required for the correct interpretation of the displayed images.

Acknowledgement—The authors gratefully acknowledge Drs. K. Kirk Shung and Ihyuan Kuo of the Bioengineering Program of Pennsylvania State University for collaborating in measuring the beam profile of the Doppler ultrasonic probe. Acknowledgments are also addressed to Mr. Richard Cimon for designing the strangling devices used to create the stenoses. Mrs. Cimon, Claude Benoit and Luc Dandeneau also provided technical assistance. The authors thank Dr. Craig Hartley at Baylor College of Medicine, Houston, Texas, for providing information that helped in evaluating the frequency response of the Doppler flowmeter.

This work was supported by a research scholarship from the Fonds de la Recherche en Santé du Québec and by a grant from the Medical Research Council of Canada (#MA-11740).

REFERENCES

- Akaike, H. A new look at the statistical model identification. *IEEE Trans. Automatic Control* AC-19:716–723; 1974.
- Bascom, P. A. J.; Routh, H. F.; Cobbold, R. S. C. Interpretation of power changes in Doppler signals from human blood—in vitro studies. *Ultrasonics Symp.* 2:985–988; 1988.
- Bascom, P. A. J.; Cobbold, R. S. C.; Routh, H. F.; Johnston, K. W. On the Doppler signal from a steady flow asymmetrical stenosis model: Effects of turbulence. *Ultrasound Med. Biol.* 19:197–210; 1993.
- Berger, N. E.; Lucas, R. J.; Twersky, V. Polydisperse scattering theory and comparisons with data for red blood cells. *J. Acoust. Soc. Am.* 89:1394–1401; 1991.
- Clark, C. The propagation of turbulence produced by a stenosis. *J. Biomech.* 13:591–604; 1980.
- Clark, C.; Schultz, D. L. Velocity distribution in aortic flow. *Cardiovasc. Res.* 7:601–613; 1973.
- Cloutier, G.; Shung, K. K. The effect of turbulence on the variation of the ultrasonic Doppler amplitude within the cardiac cycle. *Proc. 14th Conf. IEEE-EMBS* 5:2118–2119; 1992.
- Cloutier, G.; Shung, K. K. Cyclic variation of the power of ultrasonic Doppler signals backscattered by polystyrene microspheres and porcine erythrocyte suspensions. *IEEE Trans. Biomed. Eng.* 40:953–962; 1993a.
- Cloutier, G.; Shung, K. K. Study of red cell aggregation in pulsatile flow from ultrasonic Doppler power measurements. *Biorheology* 30:443–461; 1993b.
- Dacie, J. V. S.; Lewis, S. M. *Practical haematology*. Edinburgh: Churchill Livingstone; 1991.
- Evans, D. H.; McDicken, W. N.; Skidmore, R.; Woodcock, J. P. *Doppler ultrasound. Physics, instrumentation, and clinical applications*. Chichester: Wiley, 1989.
- Falsetti, H. L.; Carroll, R. J.; Swope, R. D.; Chen, C. J.; Cramer, J. A.; Length, R. A.; Laughlin, D. E. Turbulent blood flow in the ascending aorta of dogs. *Cardiovasc. Res.* 17:427–436; 1983.
- Garbini, J. L.; Forster, F. K.; Jorgensen, J. E. Measurement of fluid turbulence based on pulsed ultrasound techniques. Part I. Analysis. *J. Fluid Mech.* 118:445–470; 1982a.
- Garbini, J. L.; Forster, F. K.; Jorgensen, J. E. Measurement of fluid turbulence based on pulsed ultrasound techniques. Part 2. Experimental investigation. *J. Fluid Mech.* 118:471–505; 1982b.
- Giddens, D. P.; Zarins, C. K.; Glagov, S. The role of fluid mechanics in the localization and detection of atherosclerosis. *J. Biomech. Eng.* 115:588–594; 1993.
- Guo, Z.; Durand, L. G.; Lee, H. C. Comparison of time-frequency distribution techniques for analysis of simulated Doppler ultrasound signals of the femoral artery. *IEEE Trans. Biomed. Eng.* 41:332–342; 1994.
- Hanai, S.; Yamaguchi, T.; Kikkawa, S. Turbulence in the canine ascending aorta and the blood pressure. *Biorheology* 28:107–116; 1991.
- Jones, S. A. Fundamental sources of error and spectral broadening in Doppler ultrasound signals. *CRC Crit. Rev. Biomed. Eng.* 21:399–483; 1993.
- Kaluzynski, K. Analysis of application possibilities of autoregressive

- modelling to Doppler blood flow signal spectral analysis. *Med. Biol. Eng. Comput.* 25:373–376; 1987.
- Munter, W. A.; Stein, P. D. Turbulent blood flow and the effects of erythrocytes. *Cardiovasc. Res.* 8:338–346; 1974.
- Sabbah, H. N.; Stein, P. D. Effect of erythrocytic deformability upon turbulent blood flow. *Biorheology* 13:309–314; 1976.
- Schneck, D. J. On the development of a rheological constitutive equation for whole blood. College of Engineering, Virginia Polytechnic Institute (Tech. Rep. No. VPI-E-88-14). 1988: 1–17.
- Shung, K. K.; Yuan, Y. W.; Fei, D. Y.; Tarbell, J. M. Effect of flow disturbance on ultrasonic backscatter from blood. *J. Acoust. Soc. Am.* 75:1265–1272; 1984.
- Shung, K. K.; Cloutier, G.; Lim, C. C. The effects of hematocrit, shear rate, and turbulence on ultrasonic Doppler spectrum from blood. *IEEE Trans. Biomed. Eng.* 39:462–469; 1992.
- Shung, K. K.; Kuo, I. Y.; Cloutier, G. Ultrasonic scattering properties of blood. In: Roelandt, J.; Gussenhoven, E. J.; Bom, N., eds. *Intravascular ultrasound*. Dordrecht: Kluwer, 1993:119–139.
- Stein, P. D.; Sabbah, H. N. Contribution of erythrocytes to turbulent blood flow. *Biorheology* 12:293–299; 1975.
- Strandness, D. E., Jr. *Duplex scanning in vascular disorders*. New York: Raven Press; 1990.
- Twersky, V. Low-frequency scattering by mixtures of correlated nonspherical particles. *J. Acoust. Soc. Am.* 84:409–415; 1988.
- Vaitkus, P. J.; Cobbold, R. S. C.; Johnston, K. W. A comparative study and assessment of Doppler ultrasound spectral estimation techniques Part II: Methods and results. *Ultrasound Med. Biol.* 14:673–688; 1988.
- Young, D. F. Fluid mechanics of arterial stenoses. *J. Biomech. Eng.* 101:157–175, 1979.